

25th ABCM International Congress of Mechanical Engineering
October 20-25, 2019, Uberlândia, MG, Brazil

COB-2019-1655

DEVELOPMENT OF A COMPUTATIONAL STUDY ON A DRYING EQUIPMENT

Eng. Eduardo Dal Piva Schuch

Eng. Magaiver Gabriel Lamp

Feevale University, ERS-239, 2755, Novo Hamburgo, Brazil
eduardodpschuch@gmail.com; maguiglamp@gmail.com

Mateus Guilherme Hartmann

Feevale University, ERS-239, 2755, Novo Hamburgo, Brazil
mateus.hartmann@hotmail.com

Eng. Ismael Nicholas Schröer

Feevale University, ERS-239, 2755, Novo Hamburgo, Brazil
ismael.schroer@higra.com.br

Dra. Eng. Ângela Beatrice Dewes Moura

Feevale University, ERS-239, 2755, Novo Hamburgo, Brazil
angelab@fevale.br

Abstract. *Computational simulation software have been gaining ground in industrial and academic environments due to their potential in providing data about the functioning of equipment and processes. This study was designed to perform a numerical study through COMSOL Multiphysics software in a drying equipment used in a production line of a manufacturing industry. Two numerical models were developed in order to contemplate the radiation generated by a resistor and the movement of a test piece, simulating the conditions of the real process. The models distinguish from each other in the strategy related to the boundary conditions applied: the first model was designed by applying temperatures as boundary conditions which were measured in the real process, while the second model would calculate these temperatures instead, based on the power measured in the real process. The main objective of this study was to compare how the two numerical models would perform in terms of accuracy to the real process, being both models validated by obtaining a mean squared error of 2.49 % and 2.74 % to the first and second models, respectively. Therefore, the study concluded that the first model would be more precise, although the difference is small.*

Keywords: *numerical study, thermal radiation, computer-aided engineering.*

1. INTRODUCTION

Computer-aided engineering is a great tool to aid engineers in dealing with all kinds of analysis required in the development of projects or in the resolution of problems they might face in industrial and academic environments. Its usage, however, requires a fair understanding of the physics behind the processes being simulated and the lack of this theoretical ground will often add inaccuracies to the outcome of the simulations. Every study will require a starting point, and for studies related to an analysis for improvement of an existing equipment or process this starting point will usually require measurements of real data. The risk of inaccuracies can induce engineers into measuring as much data in the real process as possible and applying those in the numerical model. Although this seems like a safe proposal, the numerical model may be left bound to the specific scenario being simulated at the time and inapt to evaluate changes in the process (e.g., if the different temperatures of a heater in thermal equilibrium are measured and applied to a numerical model, it is able to simulate the heating of a test piece with great accuracy in those conditions, but won't be able to evaluate changes such as in power, materials and dimensions, as changing those would most likely change the temperatures that were once measured).

Therefore, in the need of simulating a process in a very specific scenario, where the "binding measurements" previously mentioned could be applied, knowing beforehand how much more accuracy (if any) could be achieved by setting a whole numerical model bound to a specific condition can be very advantageous: if it was found that the improvement is small the engineer could be spared of having to create a whole new "not bound" numerical model just to simulate changes and, instead, create this model in the first place and also use it in the very specific scenario early

mentioned, saving a fair amount of time and effort. The main objective of this study was to develop both of these possibilities for numerical models and compare how they perform in terms of accuracy to the real process.

Overall, radiation has been a subject of increasing interest. Kumar et. al. (2011) studied, experimentally, the curing of a glass fiber reinforced polymer compound through radiation as an alternative to the conventional convective method and found that not only it increases energy efficiency, but also results in a volumetric curing, thus more uniform and with lower levels of internal stresses. Similarly, Allanic et. al. (2014) studied experimentally the curing of water-based varnishes through a radiation method and established a mathematical model to simulate the process, comparing experimental and simulated results, concluding that the simulated and experimental temperatures presented good enough proximity. Severijns et. al. (2017) performed a numerical study through COMSOL Multiphysics software, but in a process involving curing by induction of adhesively bonded joints. Comparing both simulated and experimental results, the authors obtained a proximity between simulated and experimental temperatures of 15 %. Nakouzi et. al. (2011) also utilized COMSOL Multiphysics software to perform a numerical study and simulate the heat flux in the top surface of a carbon fiber reinforced epoxy matrix, comparing simulated temperatures with experimental measures and eventually obtaining a mean squared error of around 4 %.

These four articles denote the importance of studies involving radiation and numerical methods in the present, and the work done by Nakouzi et. al. (2011) shows how these two can be used together to simulate data involving radiation with great precision.

2. RADIATION DRYING

Incropera et. al. (2014) define thermal radiation as the energy emitted by matter at a nonzero temperature, explaining that every body with a finite temperature will, therefore, emit radiation. Bejan (1996) explains that the emitted radiation can interact with matter in certain ways, one of them is by being absorbed; absorption is, essentially, the process that allows heat transfer by thermal radiation. Howell et. al. (2011) further expand the subject by explaining how radiation can act as a volumetric phenomenon. They state that absorption can occur not only in the surface of bodies but also in their inner layers, leading to a more uniform heating of the body absorbing radiation. In contrast, when heat is being transferred by thermal diffusion (conduction or convection), the energy will always be transferred from the outside to the inside of a body.

According to Talbert (2008), this volumetric heating is one of the advantages of working with radiation drying. Depending on what material is being processed, the volumetric drying provided by radiation can achieve a higher product quality that could not be achieved by thermal diffusion.

2.1 Numerical methods for radiation

There are several ways to deal with radiation problems in computational simulation, and the suitability of each different method greatly depends on the circumstances of the study. According to Rey (2006), the simplest scenario occurs when the medium can be considered transparent, allowing the use of a method that deals with radiation as a surface-to-surface phenomenon, such as the radiosity-irradiosity method (RIM). In this method, all the surfaces are considered diffuse (i.e., radiation is emitted and reflected equally in all directions) and radiation exchange is based in calculating sets of geometrical entities, known as view factors, which represent the fraction of energy that is emitted by one surface and intercepted by others, for every surface in the numerical model.

3. METHODOLOGY

The equipment used as the object of this analysis is a common equipment in a production line of a manufacturing industry. In this equipment, the materials to be processed are put in a conveyor belt that crosses the interior of the equipment, receiving the load of radiation required for the drying to occur. Many configurations of crossing times can be set, therefore, three different crossing times were chosen: 30, 60 and 90 seconds.

The numerical models were developed with the use of COMSOL Multiphysics software, version 5.3a, whose license is held by Feevale University. The radiation transfer was evaluated by the RIM, as the medium consists of atmospheric air, which can safely be considered transparent. The reason why it is safe to use a surface-to-transfer method for a radiation drying process, in which the energy absorption is mostly volumetric, is due to the thickness of material being dried, which is very thin. For the radiation drying of a thick material, the RIM should not be applied.

The same situation was tested both numerically and experimentally, in which a test piece crossed the interior of the equipment. The numerical models were developed to follow the same characteristics of the experimental tests, including dimensions, materials, physical quantities and the movement of the test piece inside the equipment, by the use of a moving mesh physics. Simulations were made using all of the three crossing times, allowing for a greater analysis of accuracy, as the results can be compared in three different occasions. An illustration of the situation tested both numerically and experimentally is shown in Fig 1.

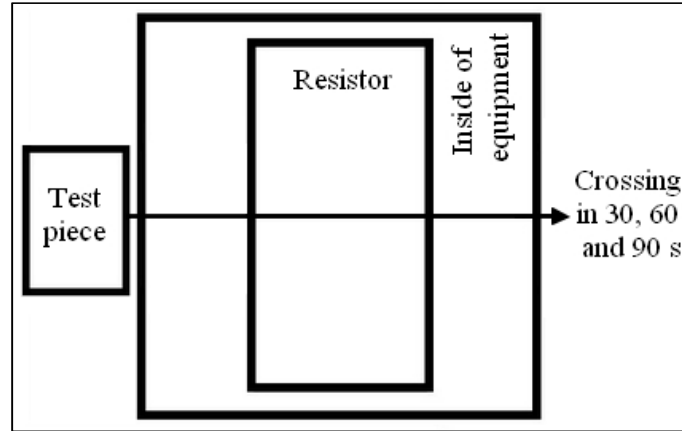


Figure 1. Illustration of the test executed numerically and experimentally.

The main physical quantity analyzed in the simulation was the temperature of the test piece, as this quantity was the biggest responsible for the drying to occur. The validation of both numerical models was performed following the method applied by Nakouzi et. al. (2011), by calculating the mean squared error, as shown in Eq. (1), where $T_{i,exp}$ are the temperatures measured in the center of the test piece in the real process, $T_{i,num}$ are the temperatures simulated in the center of the test piece in the numerical models and MSE stands for the mean squared error.

$$MSE = \left[\frac{\sum_{i=1}^n (T_{i,exp} - T_{i,num})^2}{\sum_{i=1}^n (T_{i,exp})^2} \right] * 100 \quad (1)$$

Even though this study validates the numerical models by comparing them with experimental data, a mesh study was also executed to select a mesh configuration that would provide a balance between accuracy and resource usage.

In order to develop both models, a fair amount of data was measured in the equipment during functioning. Boundary conditions applied in both numerical models consisted of emissivities and convective heat fluxes. As these quantities are impractical to measure with accuracy, initial values were obtained from the literature and those were further refined with the simulations themselves, by performing an extensive number of simulations in a wide range of values and choosing the ones that fit the most when comparing resulting simulated temperatures in the test piece with measured temperatures in the real process. Evidently, this whole method of finding values can add inaccuracies to the resolutions in relation to the real process, but as this method was applied to both models, it should not affect the comparison between the two models, which is the main objective of this study.

Once the values for the emissivities and convective heat fluxes were defined (i.e., the boundary conditions that are common to both models), the boundary conditions exclusive to the first numerical model were established. They consisted in a number of different temperatures along the different parts of the equipment, except for the resistor. In order to simulate the resistor, a different strategy was applied. Knowing that the equipment operated in thermal equilibrium, it was evident that the incoming power would be equal to the outgoing power. In other words, the power measured in the resistor by multiplying voltage and electric current would be equal to the energy it was releasing per second (i.e., no energy absorbed by the resistor). Therefore, measuring the current and the voltage to calculate power and also measuring the superficial area of the resistor would result in a value for energy flux, which was used as a prescribed radiosity. Utilizing this method to simulate the resistor spared the need of applying an emissivity and a convective heat flux to it.

The boundary conditions exclusive to the second numerical model were an emissivity and a convective heat flux in the resistor and a boundary heat source equal to the power measured by multiplying voltage and current. All temperature constraints applied in the first numerical model, which bound it to a specific scenario, were removed, resulting in a numerical model apt to test changes in the process. In order to simulate an equipment in thermal equilibrium, all the materials of its domains had their specific heat set to 0.001 J/kgK, except for the test piece, for which the original material specific heat was maintained. By doing so, the amount of energy consumed by the components of the equipment to reach thermal equilibrium is negligible, while the test piece will still require as much energy to raise its temperature as it should.

After validating both numerical models, a deeper comparison was performed between them. The progression of temperatures in the center of the test piece during the process for both numerical models was analyzed in the three crossing times, observing how the heating differed for each model. By doing so, two curves were obtained for every crossing time, one for the first model and one for the second model, making possible a graphic comparison. Later, the test piece was visually analyzed for every occasion (i.e., both numerical models, all three crossing times) in order to check temperature distribution in all the extension of the test piece. Finally, a thermal photograph of an experimental test with a crossing

time of 90 s was captured, allowing for a comparison of both numerical models with the experimental model for this situation. The thermal camera is capable of identifying the highest temperature in the test piece; therefore, this information was also obtained in both numerical models for a crossing time of 90 s.

4. RESULTS AND DISCUSSION

In the mesh study, a mesh configuration of 2,582 tetrahedral elements was selected. This was the configuration used in every study performed, for both numerical models.

The temperatures measured in the center of the test piece for both numerical models are shown in Tab. 1, together with the temperatures obtained by executing the tests experimentally.

Table 1. Experimental and simulated temperatures for both numerical models.

Time (s)	Temperatures in the center of the test piece (°C)		
	Real process	First numerical model	Second numerical model
30	93	89.97	89.76
60	116	119.46	120.33
90	135	136.95	133.96

With the results shown in Tab. 1, the mean squared error was calculated for each of them by utilizing Eq. (1), resulting in the values presented in Tab. 2.

Table 2. Mean squared error for each numerical model.

Numerical model	Mean squared error (%)
First	2.49
Second	2.74

By analyzing the values in Tab. 2, it can be noticed that the overall inaccuracies were found to be considerably small. As mentioned earlier, Severijns et. al. (2017) and Nakouzi et. al. (2011) obtained inaccuracies of around 15 % and 4 %, respectively, indicating that the methods applied for both numerical models in this study had a great similarity to the real process being simulated. The first numerical model resulted in a higher accuracy than the second numerical model, but the difference between both was considerably small. However, it's worth to notice that for a crossing time of 90 s, the second numerical model presented a higher accuracy than the first one.

After concluding the validation, the next step was to compare temperature development between both numerical models in the three chosen crossing times. The progression of temperatures for both numerical models with crossing time of 30 s is presented in Fig. 2.

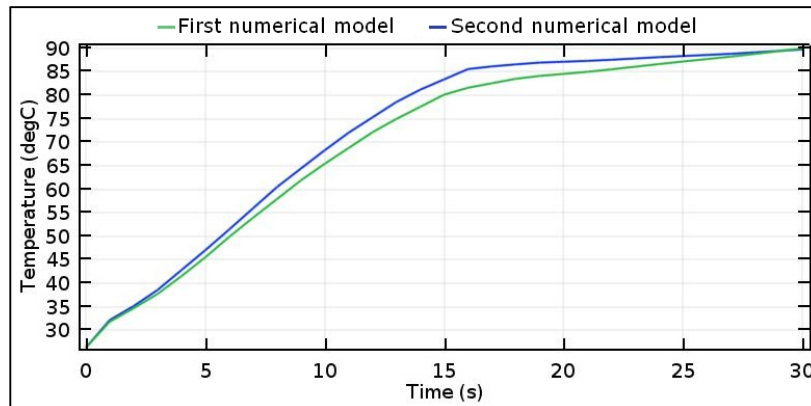


Figure 2. Progression of temperatures in the center of the test piece for both numerical models with a crossing time inside the equipment of 30 s.

Figure 2 shows that the second model reached higher temperatures faster than the first model during the heating of the test piece, although the final temperature at 30 s is higher in the first model than in the second. The overall behavior is similar for both models: the temperature kept increasing until the end of the process, reaching peak temperature at the time of 30 s.

The progression of temperatures for a crossing time inside the equipment of 60 s is shown in Fig. 3.

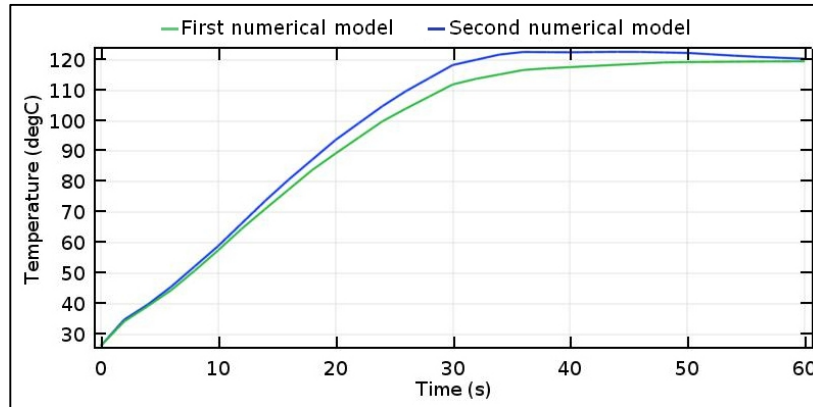


Figure 3. Progression of temperatures in the center of the test piece for both numerical models with a crossing time inside the equipment of 60 s.

Again, Fig. 3 shows that in the second model the test piece reached higher temperatures faster than in the first model during the heating process, but this time it can be seen that the overall behavior is different: in the first model, the temperature in the center of the test piece kept increasing until the end of the process, while in the second model it reached peak temperature at around 35 s and decreased from that point.

Finally, Fig. 4 presents the progression of temperatures in the center of the test piece for a crossing time of 90 s.

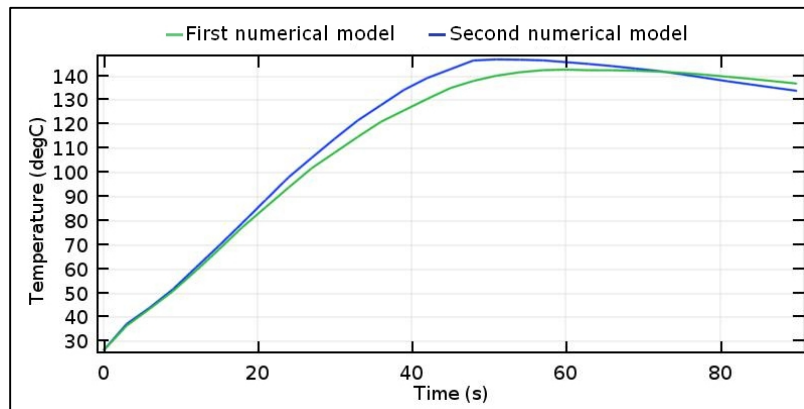


Figure 4. Progression of temperatures in the center of the test piece for both numerical models with a crossing time inside the equipment of 90 s.

As seen in Fig 4, in both models a maximum temperature was reached during the process, followed by a continuous decrease which was higher in the second numerical model, where the peak temperature was achieved earlier. Temperature development in the center of the test piece in the second model resulted in a higher heating when compared to the first model. The fact that this was a pattern obtained in all three crossing times indicates that this is an intransient behavior, and the same can be said for the cooling of the test piece, as for a crossing time of 60 s a temperature decrease was seen only in the second model and for a crossing time of 90 s the temperature decrease was bigger in the second model than in the first one. In short, the test piece heated and cooled faster in the second numerical model and slower in the first numerical model.

The next step in the study was to visually analyze the test piece after it exited the equipment, comparing the temperature distribution in both numerical models. Figure 5 shows this comparison for a crossing time of 30 s.

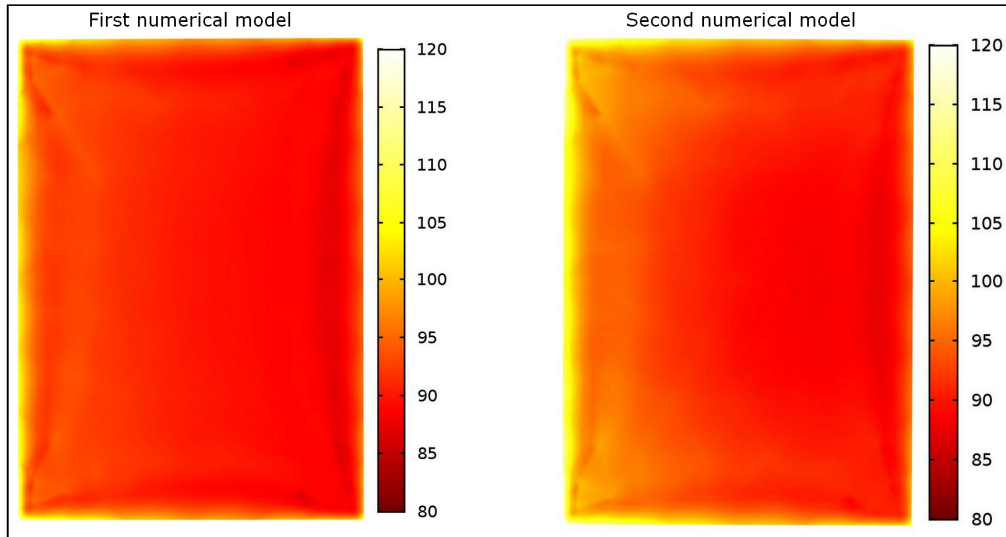


Figure 5. Temperature distribution in the test piece for both numerical models with a crossing time inside the equipment of 30 s.

There are two major differences that can be spotted in Fig. 5. The first is how differently temperature was distributed in each model; the first model appeared to be more homogeneous than the second. The second difference was in the edges of the test piece. Numerical errors are more likely to occur in mesh edges, which in this case would result in temperatures that differ from reality. It's possible to notice in Fig. 5 that in both models there was a concentration of higher temperatures in the edges, but in the second model this concentration was more expressive. Both of these two differences could be an indicative that numerical errors were larger in the second model.

Temperature distribution for a crossing time of 60 s is presented in Fig. 6.

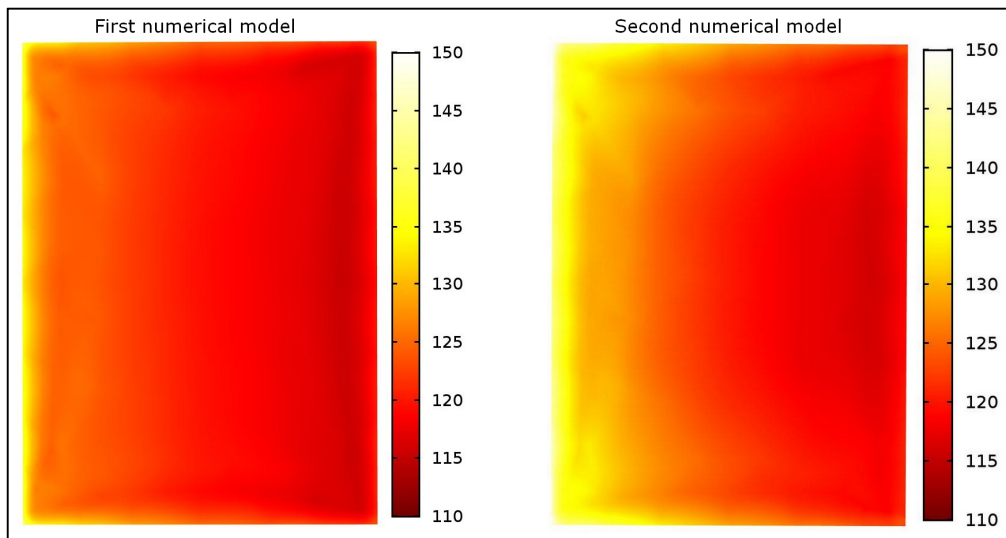


Figure 6. Temperature distribution in the test piece for both numerical models with a crossing time inside the equipment of 60 s.

It can be seen in Fig. 6 that the concentration of higher temperature in the edges no longer existed, the gradient of temperature depended mostly on which side of the test piece left the insides of the equipment first. This may indicate that the numerical studies with a crossing time of 60 s were more precise. It's also still clear that the overall temperatures in the second numerical model were higher.

Last, the temperature distribution in the test with a crossing time of 90 s is shown in Fig. 7, where the maximum temperature in the test piece is also included.

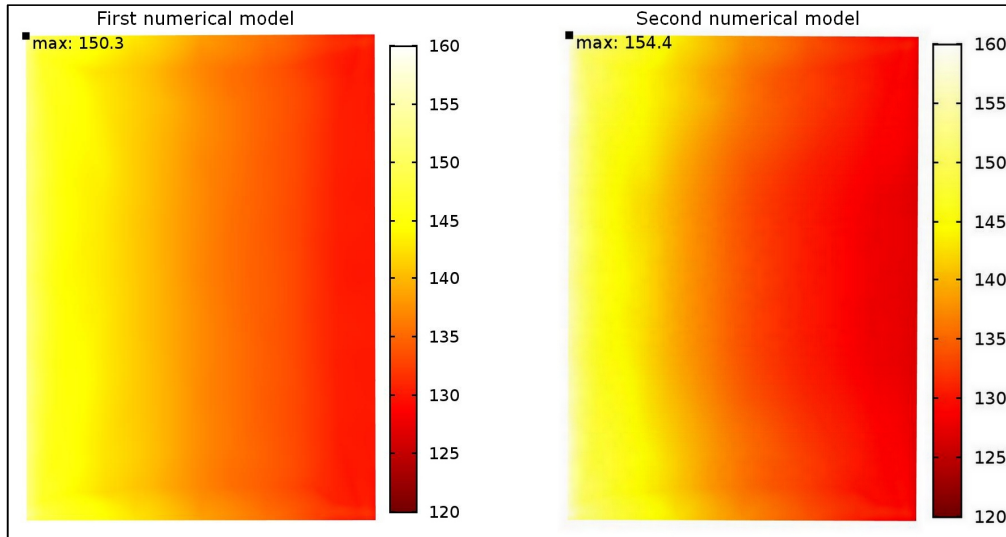


Figure 7. Temperature distribution and maximum temperature in the test piece for both numerical models with a crossing time inside the equipment of 90 s.

Figure 7 makes clear that for a crossing time of 90 s the temperature distribution in the test piece was the smoothest, possibly indicating that this scenario provided the highest accuracy among all three. The temperature in the center of the test piece, as seen is Tab. 1, was lower in the second model and closer to the temperature measured in the experimental model for this scenario. The highest achieved temperature at the exit, however, was higher in the second model by around 4.1 °C. For a greater comparison, Fig. 8 presents a thermal photograph captured in the experimental model for a crossing time of 90 s.

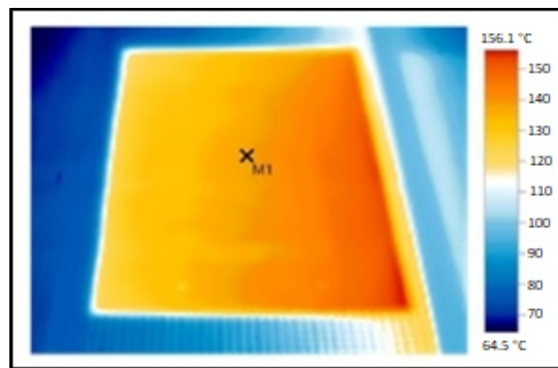


Figure 8. Thermal capture of the test piece in the experimental model after exiting the inside of equipment with a crossing time of 90 s.

As seen in Fig. 8, the highest temperature in the test piece after leaving the equipment with a crossing time of 90 s was around 156.1 °C, which is, again, closer to the value obtained in the second numerical model. It's worth to notice that the trajectory of the test piece was inverted in Fig 8. While in Fig. 5, Fig. 6 and Fig. 7 the path was from left to right, in Fig. 8 the path was from right to left.

5. CONCLUSION

Many conclusions can be made and speculated after analyzing the results. By the MSE shown in Tab. 2, the first model proved to be more precise than the second model, although the inaccuracies of the second numerical model were roughly 10 % bigger when compared to the first model. However, analyzing the temperature development in the center of the test piece during the heating process revealed that the difference was greater around the middle of the heating process than at its end. The figures of temperature distribution also contributed to this observation, showing that even though the temperatures in the center of the test piece after exiting the inside of the equipment were close, there was a bigger difference in other regions of the test piece for all crossing times. These facts demonstrated that numerical models

can diverge in the middle of a process and still give similar results at the end; therefore, when in a situation where a very high accuracy is needed, the investigation the engineer performs to experimentally validate the numerical model should be more detailed than only measuring outputs.

The temperatures presented in Tab. 1 demonstrate that for crossing times of 30 and 60 s the first model resulted in more accurate temperatures, while the opposite was true for a crossing time of 90 s. The max temperature obtained in both numerical models in Fig. 7 and in the experimental model in Fig. 8 also contributed to this, as the temperature of 154.4 °C for the second numerical model was closer to the 156.1 °C of the experimental model than the 150.3 °C obtained in the first numerical model.

By comparing temperature distribution in the test piece for the three crossing times tested, the results demonstrated that higher crossing times resulted in smoother temperature distributions, possibly indicating that the accuracy was proportional the amount of time spent in the path of a moving mesh, which means that increasing the crossing time could have a result similar to increasing mesh refinement. This relation was also supported by the higher accuracy obtained in the second numerical model for a crossing time of 90 s. The numerical calculations executed in this model were bigger than in the first model due to the bigger amount of equations it possessed, consequently increasing the mesh quality dependence of the second numerical model. Refining the mesh, however, can severely impact the amount of computational resources needed and the time taken for a simulation to converge, while the impact of increasing the crossing time was close to none in this study. This information, if confirmed, could be remarkably advantageous to the engineer, as it may consist of a method to obtain more accurate results without significantly increasing computational resources needed, for a study similar to the one executed in this paper. A suggestion for future works is to investigate this phenomenon and check its legitimacy.

Overall, it can be concluded that both numerical models were validated and resulted in a great accuracy when compared to the experimental model. Therefore, for most situations, an engineer in charge of creating a computational heat transfer study in similar condition can build an unbound model, able to evaluate changes, and execute all the necessary studies from it.

6. REFERENCES

- Allanic, N., Bideau, P. L., Glouannec, P. and Bourmaud, A., 2014. "Infrared drying of water based varnish coated on elastomer substrate". *International Journal of Thermal Science*, Vol. 79, pp. 103-110.
- Bejan, A., 1996. *Transferência de calor*. Edgard Blücher, São Paulo.
- Howell, J. R., Mengüç, M.P. and Siegel R., 2015. *Thermal Radiation Heat Transfer*. CRC Press, Boca Raton, 6th edition.
- Incropera, F.P., DeWitt, D.P., Bergman, T.L. and Lavine, A.S., 2011. *Fundamentals of Heat and Mass Transfer*. John Wiley & Sons, Hoboken, 7th edition.
- Kumar, P. K., Raghavendra, N. V. and Sridhara, B. K., 2011. "Optimization of infrared radiation cure process parameters for glass fiber". *Materials and Design*, Vol. 32, No. 3, pp. 1129-1137.
- Nakouzi, S., Berthet, F., Maoult, Y. L. and Schmidt, F., 2011. "Simulations of an infrared composite curing process". *Advanced Engineering Material*, Vol. 13, No. 7, pp. 604-608.
- Rey G. C., 2006. *Numerical methods for radiative heat transfer*. Ph.D. thesis, Universitat Politècnica de Catalunya, Terrassa, Spain.
- Severijns, C., Freitas, S. T. and Poulis, J. A., 2017. "Susceptor-assisted induction curing behaviour of a two component epoxy paste adhesive for aerospace applications". *International Journal of Adhesion and Adhesives*, Vol. 75, pp. 155-164.
- Talbert, R., 2008. *Paint technology handbook*. Taylor & Francis Group, Boca Raton.

7. RESPONSIBILITY NOTICE

The authors are the only responsible for the printed material included in this paper.